Acta Pharmaceutica Sinica B 2023;13(7):2976–2989

Chinese Pharmaceutical Association
Institute of Materia Medica, Chinese Academy of Medical Sciences

Acta Pharmaceutica Sinica B

www.elsevier.com/locate/apsb
www.sciencedirect.com

ORIGINAL ARTICLE

GPRC5B protects osteoarthritis by regulation of autophagy signaling

Liang He[a,†], Ziwei Xu[b,†], Xin Niu[b,†], Rong Li[a], Fanhua Wang[a], Yu You[b], Jingduo Gao[b], Lei Zhao[a], Karan M. Shah[c], Jian Fan[d,*], Mingyao Liu[b,*], Jian Luo[a,*]

[a]*Yangzhi Rehabilitation Hospital (Shanghai Sunshine Rehabilitation Center), Tongji University School of Medicine, Shanghai 201613, China*
[b]*Shanghai Key Laboratory of Regulatory Biology, Institute of Biomedical Sciences and School of Life Sciences, East China Normal University, Shanghai 200241, China*
[c]*Department of Oncology and Metabolism, the Medical School, the University of Sheffield, Sheffield S10 2TN, UK*
[d]*Department of Orthopedics, Tongji Hospital, Tongji University School of Medicine, Shanghai 200092, China*

Received 30 November 2022; received in revised form 17 January 2023; accepted 14 March 2023

KEY WORDS

Osteoarthritis;
GPRC5B;
Cartilage;
Chondrocyte;
Cartilage anabolism and catabolism;
Cartilage regeneration;
Autophagy;
Drug target

Abstract Osteoarthritis (OA) is one of the most common chronic diseases in the world. However, current treatment modalities mainly relieve pain and inhibit cartilage degradation, but do not promote cartilage regeneration. In this study, we show that G protein-coupled receptor class C group 5 member B (GPRC5B), an orphan G-protein-couple receptor, not only inhibits cartilage degradation, but also increases cartilage regeneration and thereby is protective against OA. We observed that *Gprc5b* deficient chondrocytes had an upregulation of cartilage catabolic gene expression, along with downregulation of anabolic genes *in vitro*. Furthermore, mice deficient in *Gprc5b* displayed a more severe OA phenotype in the destabilization of the medial meniscus (DMM) induced OA mouse model, with upregulation of cartilage catabolic factors and downregulation of anabolic factors, consistent with our *in vitro* findings. Overexpression of *Gprc5b* by lentiviral vectors alleviated the cartilage degeneration in DMM-induced OA mouse model by inhibiting cartilage degradation and promoting regeneration. We also assessed the molecular mechanisms downstream of *Gprc5b* that may mediate these observed effects and identify the role of protein kinase B (AKT)-mammalian target of rapamycin (mTOR)-autophagy signaling pathway. Thus, we demonstrate an integral role of GPRC5B in OA pathogenesis, and activation of GPRC5B has the potential in preventing the progression of OA.

*Corresponding authors.
E-mail addresses: qidongfanjian@sina.com (Jian Fan), myliu@bio.ecnu.edu.cn (Mingyao Liu), jluo@tongji.edu.cn (Jian Luo).
[†]These authors made equal contributions to this work.
Peer review under the responsibility of Chinese Pharmaceutical Association and Institute of Materia Medica, Chinese Academy of Medical Sciences.

https://doi.org/10.1016/j.apsb.2023.05.014

1. Introduction

OA is a common joint disease that is characterized by cartilage degeneration and synovial hypertrophy, and is associated with significant pain and morbidity. Between 2010 and 2019, the global prevalence of osteoarthritis and the resulting disability have risen by 27.5%[1], and as of 2019 OA is estimated to affect 528 million people worldwide and is the 15th leading cause of disability[2]. OA can affect all joint tissues, and leads to joint dysfunction, pain, and organismal changes that reduce the quality of life, initiate or aggravate co-morbidities, and reduce life expectancy[3]. Indeed, OA-mediated reduction in physical activity results in a mortality ratio of 1.55% in its patient population[4]. The current treatment options for OA mainly relieve pain, and have little effect on the prevention of cartilage degeneration, and therefore joint replacement for end-stage disease remains the only long-term treatment option[5]. Therefore, there is an urgent need to identify novel therapeutic targets that can prevent or delay the progression of this disease[5].

Whilst the clinical and socioeconomic impacts of OA are well known, our understanding of its genetic basis is in its infancy. Accelerating gene discovery in osteoarthritis will increase understanding of joint physiology and disease pathogenesis and facilitate identification of drug targets. G protein-coupled receptors (GPCRs) are seven-transmembrane helix receptors which make the largest family of transmembrane proteins and are critical components of several fundamental biological processes[6]. GPCRs remain the most widely researched targets for drug discovery and make up to 30% of targets for US Food and Drug Administration (FDA) approved drugs[7,8]. GPCRs play an integral role in bone development and remodeling and several bone diseases have been associated with GPCR function[9].

GPRC5B is an orphan GPCR which has been shown to have associations with psychiatric conditions[10], obesity and cardiometabolic diseases[11]. Furthermore, increased GPRC5B expression was associated with reduced insulin secretion[12]. GPRC5B has also been shown to play a role in inflammation by facilitating macrophage infiltration and inflammatory cell recruitment through the nuclear factor-κ-gene binding (NF-κB) signaling pathways[13,14]. Additionally, decreased GPRC5B expression has been linked to neuropathic pain *in vivo*[15] with GPRC5B playing a role in inflammation *via* NF-κB which is implicated in OA pathophysiology[16–18], as well as pain which is also a characteristic of OA[19], we investigate its role in the progression of OA in this study.

2. Methods and materials

2.1. Ethics approval and consent to participate

Human and animal studies received ethical approval by the Ethic Committee of Shanghai Sixth people's hospital (2021-048) and East China Normal University (ECNU) Animal Care and Use Committee (m20200407). All patients provided written informed consent prior to their participation and in accordance to requirements of the Hospital Board. Human tissues were obtained with approval by Shanghai Sixth People's Hospital. The study design and conduct complied with all relevant regulations regarding the use of human study participants and was conducted in accordance with the criteria set by the Declaration of Helsinki. All animal studies were performed according to protocols approved by ECNU Animal Care and Use Committee. All mice were freely allowed access to food, water, and activity. Mice were maintained under a 12 h dark−light cycle and constant temperature (20−26 °C) and humidity maintenance (40%−60%).

2.2. Mice

All experiments using mice were approved by the ECNU Animal Care and Use Committee. *Gprc5b* knockout mice (*Gprc5b*$^{-/-}$) were generated by the Animal Center of ECNU using the CRISPR/Cas9 system in the C57BL/6J mouse strain. A 202-bp region was deleted from *Gprc5b* and confirmed by polymerase chain reaction (PCR) (Supporting Information Fig. S2A and S2B). C57BL/6J wide-type (WT) male mice and *Gprc5b*-deficient (*Gprc5b*$^{-/-}$, C57BL/6J) male mice were used in this study. For genotyping of *Gprc5b*$^{-/-}$ mice, PCR primer sequences for *Gprc5b* were 5′-TGAGGGTCCACAAG GTCAG-3′ (forward) and 5′-TGTCACGCAGCACAGTCAG-3′ (reverse).

2.3. Preparation of human samples

Human osteoarthritic cartilage samples were obtained from the Shanghai Sixth People's Hospital, and provided by 55 to 85-year-old patients who were undergoing joint replacement surgeries. We collected clinical samples of OA from aged patients without any traumatic injury and the basic clinical information of these patients is presented in Supporting Information Table S1. OA affected (damaged) distal medial condyle and healthy (intact) posterior lateral condyle cartilage explants were cut into pieces of about 2 mm × 5 mm. These cartilage explants were used for histological analysis or mRNA/protein expression examination.

2.4. Experimental OA in mice

Eight-week-old C57BL/6J male mice were anesthetized and the joint capsule of right knee, medial to the patellar tendon was excised. The medial menisco−tibial ligaments were cut with microsurgical bistoury. For the sham operated group, incisions were made at the knee joint without excision of any tissue. The mice were assessed for pain eight weeks following the operation, at which point the animals were sacrificed and knee joints collected for histological analysis.

2.5. Pain assay

Mice were kept in a quiet environment and allowed to acclimatize for at least 60 min. The thermal hyperalgesia of the hind paw was

estimated with the hot-plate assay (UGO 37370) as reported previously[20]. An infrared radiant heat source was directed onto the hot plate surface of the hind paw, and the withdrawal response noted as the paw withdrawal latency. The test was performed by individuals who were blinded to the experimental groups and the assessment was repeated three times for each animal.

2.6. Plasmid construction

pcDNA3.1 (+)/*Gprc5b*-expressing plasmid was constructed by inserting murine *Gprc5b* sequence into pcDNA3.1 vector amplified using: m*Gprc5b*-F (5′-AGCTTGGTACCGAGCTCGGATCATGTTCCTGGT GTTAGAGAGAAAGATGAGAACCCATCA-3′) and m*Gprc5b*-R (5′-TGCTGGATATCTGCAGAAT TTCAGAAAGCTCCAAAGGACTCCAGAG-3′) primers. pcDNA3.1 (+)/*Gprc5b*-expressing plasmid were used for following experiment. For overexpression, *Gprc5b* lentivirus were constructed by inserting murine *Gprc5b* sequence into pLVX-IRES-ZsGreen1 vector amplified using: m*Gprc5b*-F (5′-TCTAGAGCGGCCGCGG ATCCATGTTCCTGGTGTTAGAG-3′) and m*Gprc5b*-R (5′-GAG GGA GAGGGGCGGGATCCCTGCGTTAT GTTCATCCATT-3′) primers. For virus packaging, HEK293T cells were seeded in 10 cm cell culture dish at 1×10^7 cells, then transfected using polyethylenimine with pLVX-IRES-*Gprc5b* construct or pLVX-IRES-ZsGreen1 vector, and psPAX2 and pMD2G for viral envelope and capsid proteins respectively. The virus-containing culture media was harvested at 48 and 72 h. By centrifugation ($500 \times g$, 10 min, Eppendorf, China), and the filtration through 0.2 μm syringe filter. Subsequently, the supernatant was ultracentrifuged twice ($50{,}000 \times g$, 2 h each, Eppendorf, China), and resuspended in phosphate buffered saline (PBS). The viral titer was determined using 293T cells.

2.7. Intra-articular injection

For intra-articular injections, all mice that underwent DMM surgery were randomly divided into two groups: (1) vector group; (2) overexpression *Gprc5b* group. The overexpression *Gprc5b* group was intra-articular injected with pLVX-IRES-*Gprc5b* lentivirus (1×10^7 pfu in 10 μL, 5 MOI) every 4 days, and vector group controls received the pLVX-IRES-Zsgreen vector lentivirus (1×10^7 pfu in 10 μL, 5 MOI) every 4 days after DMM operation. The study was terminated 28-day post DMM surgery.

2.8. Histologic analysis

At the end of the study, the knee joints were fixed in 10% formaldehyde at 4 °C for >48 h, decalcified in 0.5 mol/L ethylene diamine tetraacetic acid (EDTA, pH 7.4) for 14 days, and embedded in paraffin. Next, the paraffin blocks were cut into 5 μm sections and stained with hematoxylin & eosin (H&E) and Safranin O according to standard procedures. The histological OA scores for medial femoral condyle, the medial tibia plateau, and summed scores for femur and tibia were evaluated using the Osteoarthritis Research Society International (OARSI) grades (0−6). Each section was scored as: 0 = normal cartilage; 0.5 = loss of Safranin O without structural changes; 1 = small fibrillations without loss of cartilage; 2 = vertical clefts down to the layer immediately below the superficial layer and some loss of surface lamina; 3 = vertical clefts/erosion to the calcified cartilage extending to <25% of the articular surface; 4 = vertical clefts/erosion to the calcified cartilage extending to 25%−50% of the articular surface; 5 = vertical clefts/erosion to the calcified cartilage extending to 50%−75% of the articular surface; 6 = vertical clefts/erosion to the calcified cartilage extending >75% of the articular surface[21]. Synovitis was evaluated according to a previously described scoring system[22].

2.9. Immunostaining

Immunohistochemistry (IHC) was performed using the Immunohistochemical kit (Miao Tong Biological), as per the manufacturer's suggestion. Briefly, paraffin sections were treated by gradient of dehydration, and then fixed in 4% polyformaldehyde (PFA) for 30 min. The tissue was permeabilized using 0.1% Triton X-100 and 0.1% phosphate-buffered saline tween (PBST) for 30 min, and antigen retrieval was performed with 20 μg/mL proteinase K for 20 min. The endogenous peroxidase activity was quenched by 3% H_2O_2, and the tissues were blocked with 2% bovine serum albumin (BSA) for 60 min. Sections were then incubated overnight at 4 °C with antibodies of Matrix Metallopeptidase 13 (MMP13, 1:100, Abcam, ab219620) or GPRC5B (1:100, Sigma, HPA015247). The sections were then washed and incubated with corresponding secondary antibodies and visualized by diaminobenzidine (DAB). The sections were counterstained by hematoxylin and images taken by Olympus microsystems microscope (Olympus Corporation, Tokyo, Japan) and counted using ImageJ software. For immunofluorescence (IF) staining, the sections were incubated overnight at 4 °C with primary antibodies for Collagen Type X Alpha 1 (COL10A1, 1:100, Abcam, ab260040), Aggrecan (ACAN, 1:100, Proteintech, 13880-1-AP) and microtubule-associated protein light chain 3 (LC3, 1:100, Proteintech, 14600-1-AP). Subsequently, the sections were washed and incubated with fluorescent secondary antibody for 1 h protected from light. Nuclei were visualized with 1 μg/mL 4,6-diamino-2-phenyl indole (DAPI, Sigma−Aldrich, D9542). Three-dimensional images were taken by Olympus fluorescence microscope (Olympus Corporation, Tokyo, Japan) and counted using ImageJ software.

2.10. Cell culture

Primary articular chondrocytes were obtained by digesting articular cartilage tissue of newborn mice (Day 3 postnatal) with 0.2% type 2 collagenase (Gibco, MA, USA). The isolated chondrocytes were maintained in DMEM/F12 (Gibco, MA, USA) supplemented with 1% penicillin/streptomycin and 10% (*v*/*v*) fetal bovine serum (Gibco, USA). ATDC5 cells were cultured in DMEM containing 10% fetal bovine serum. Mouse articular chondrocytes were stimulated with Interleukin 1β (IL-1β, R&D System, Minneapolis, MN, USA) or tumor necrosis factor alpha (TNF-α, Peprotech, USA) for the experiments in this study.

2.11. Culture of mouse femoral head

We isolated the femoral head from eight-week-old *Gprc5b*$^{-/-}$ mice and wild-type control mice, and cultured them with 10 ng/mL TNF-α for three days. Subsequently, the femoral heads were fixed in 10% formaldehyde at 4 °C for >48 h, decalcified in 0.5 mol/L EDTA in PBS (pH 7.4) for 14 days, and embedded in paraffin. Next, the paraffin blocks were cut into 5-μm sections and processed Safranin-O staining and immunostaining.

2.12. Reverse transcription and real-time quantitative PCR (RT-qPCR)

Total RNA was extracted using TRIzol reagent (Takara, 9109) from primary murine articular chondrocytes and ATDC5 cells. The RNA was Reverse-Tran scribed into complementary DNA (cDNA) using Hiscript II Q RT SuperMix (Vazyme R222-01), and real-time PCR analysis was performed using a real-time PCR system (QuantStudio Design & Analysis) with qPCR SYBR Green Master Mix (YEASEN, 11202ES03). The primers for real-time PCR were as follows:

Mouse *Mmp3*: 5′-TTGACTCAAGGGTGGATGCTGTCT-3′,
Antisense 5′-GCACATGCTGAACAAAGCACTTCC-3′;
Mouse *Mmp9*: 5′-GCCCTGGAACTCACACGACA-3′,
Antisense 5′-TTGGAAACTCACACGCCAGAAG-3′;
Mouse *Mmp13*: 5′-GTGTGGAGTTATGATGATGT-3′,
Antisense 5′-TGCGATTACTCCAGATACTG-3′;
Mouse *Sox9*: 5′-CGGCTCCAGCAAGAACAAG-3′,
Antisense 5′-GCGCCCACACCATGAAG-3′;
Mouse *Acan*: 5′-GAAGACGACATCACCATCCAG-3′,
Antisense 5′-CTGTCTTTGTCACCCACACATG-3′;
Mouse *Col2α1*: 5′-CCTCCGTCTACTGTCCACTGA-3′,
Antisense 5′-ATTGGAGCCCTGGATGAGCA-3′;
Mouse *Gprc5b*: 5′-GGAGATCCACTACACCCTTCT-3′,
Antisense 5′-GGAGAGCTGCGTTATGTTCAT-3′;
Human *GPRC5B*: 5′-CACGCCCAACTACTTCGACA-3′,
Antisense 5′-AGCTGCATTGTGTTCATCCAT-3′.

2.13. Western blotting assay

The cells were lysed using radioimmunoprecipitation assay buffer (RIPA) lysis buffer containing protease inhibitor cocktail (Roche) and phosphatase inhibitors (Roche) on ice for 15 min, the insoluble material was separated by centrifugation (12,000 rpm, 10 min, 4 °C, Centrifuge, Eppendorf, China, 5418R), and the supernatants were collected. The protein concentration was determined by bicinchoninic acid protein (Thermo Fisher Scientific). Equal amounts of protein were subjected to electrophoresis on 10% or 15% gradient sodium dodecyl sulfate-polyacrylamide gels (Bio-Rad) and transferred to nitrocellulose filter membrane (Beyotime). The membranes were blocked with 5% BSA (Beyotime) and incubated with specific antibodies, including p-AKT antibody (CST, USA, 9271, 1:1000), AKT antibody (CST, USA, 9272, 1:1000), GAPDH antibody (CST, USA, 2118, 1:10,000), p-mTOR antibody (CST, USA, 2983, 1:1000), mTOR antibody (CST, USA, 2971, 1:1000), LC3 antibody (proteintech, 14600-1-AP, 1:1000), ACAN (Proteintech, 13880-1-AP, 1:500), MMP13 (Servicebio, GB11247-1, 1:1000), SQSTM1 (Abmart, T59081XS, 1:1000), BECN1 (Abmart, T55092XS, 1:1000), GAPDH (Cell Signaling Technology; 1:10,000), and then incubated with horseradish peroxidase (HRP)-conjugated secondary antibodies (Licor 926-32211/926-32210).

2.14. Statistical analysis

Each experiment was repeated two or three times *in vitro*, analysis was performed using the Prism 7.0 software (GraphPad Prism). The data are presented as mean ± standard deviation (SD). Statistical significance of two or more groups were calculated using two-tailed Student's *t*-test or two-way ANOVA with Dunnett's test used for multiple comparisons. A P value below 0.05 was considered statistically significant.

3. Results

3.1. The expression of GPRC5B is associated with OA and inflammation

To identify key regulators of OA progression, two gene expression profile datasets for OA patients with damage and healthy cartilage were selected from Gene Expression Omnibus (GEO) and ArrayExpress. According to the established criteria for screening differentially expressed genes (DEGs), our results revealed that GSE57218 dataset contained 1893 unique DEGs compared to 1575 unique DEGs for the E-MTAB-4304 dataset (Fig. 1A). We next analyzed gene expression profile datasets of primary mouse articular chondrocytes treated with interleukin-1β from GEO, the results revealed that GSE57218 dataset contained 4742 unique DEGs. There were 27 genes identified to common for all three datasets (Fig. 1A and B). Given that GPCRs represent a major therapeutic target class and GPRC5B being the only GPCR within these 27 common genes, we focused on investigating the role of GPRC5B in OA.

We next collected human articular cartilage tissues from three OA patients undergoing total knee replacement without any traumatic joint injury. The damaged and intact cartilage explants were collected for histological analysis or for assessing mRNA/protein expression (Fig. 1C and Supporting Information Table S1). We observed that GPRC5B expression was lower in the damaged OA cartilage compared to intact cartilage by histological analysis (Fig. 1D and E). GPRC5B expression at the mRNA and protein level were observed to be lower in the damaged articular cartilage compared to intact cartilage (Fig. 1F−H). Furthermore, histological analysis showed decreased expression of GPRC5B in 24-month aged mice compared to 6-months young mice (Fig. 1I and J). Taken together, these results suggest a role of GPRC5B expression in OA pathogenesis.

To investigate whether GPRC5B expression could be affected in inflammatory conditions, we exposed the primary murine articular chondrocytes to varying concentrations of TNF-α and IL-1β. We observed that the inflammatory factors did indeed inhibit the expression of *Gprc5b* mRNA (Supporting Information Fig. S1A and S1B).

3.2. Ablation of Gprc5b aggravates OA pathogenesis in mice

We next evaluated the relationship between *Gprc5b* and OA progression by generating *Gprc5b*$^{-/-}$ mice and examining the effect in an OA murine model. We validated the establishment of a *Gprc5b*$^{-/-}$ mouse line confirming the lack of mRNA and protein expression of GPRC5B (Fig. S2C−S2E). After 8 weeks of DMM surgery, the cartilage damage was significantly aggravated in *Gprc5b*$^{-/-}$ mice compared to the littermate wild-type controls (Fig. 2A). Microscopic scoring also showed articular cartilage damage was significantly aggravated in the medial tibia plateau (MTP) and medial femoral condyle (MFC) in the *Gprc5b*$^{-/-}$ mice compared to the wild-type controls (Fig. 2B−D), and was associated with increased osteophyte development in *Gprc5b*$^{-/-}$ mice (Supporting Information Fig. S3A and S3B). Pain withdrawal threshold was also lower in *Gprc5b*$^{-/-}$ mice compared to wild-type controls, following DMM-induced OA (Fig. 2E). However,

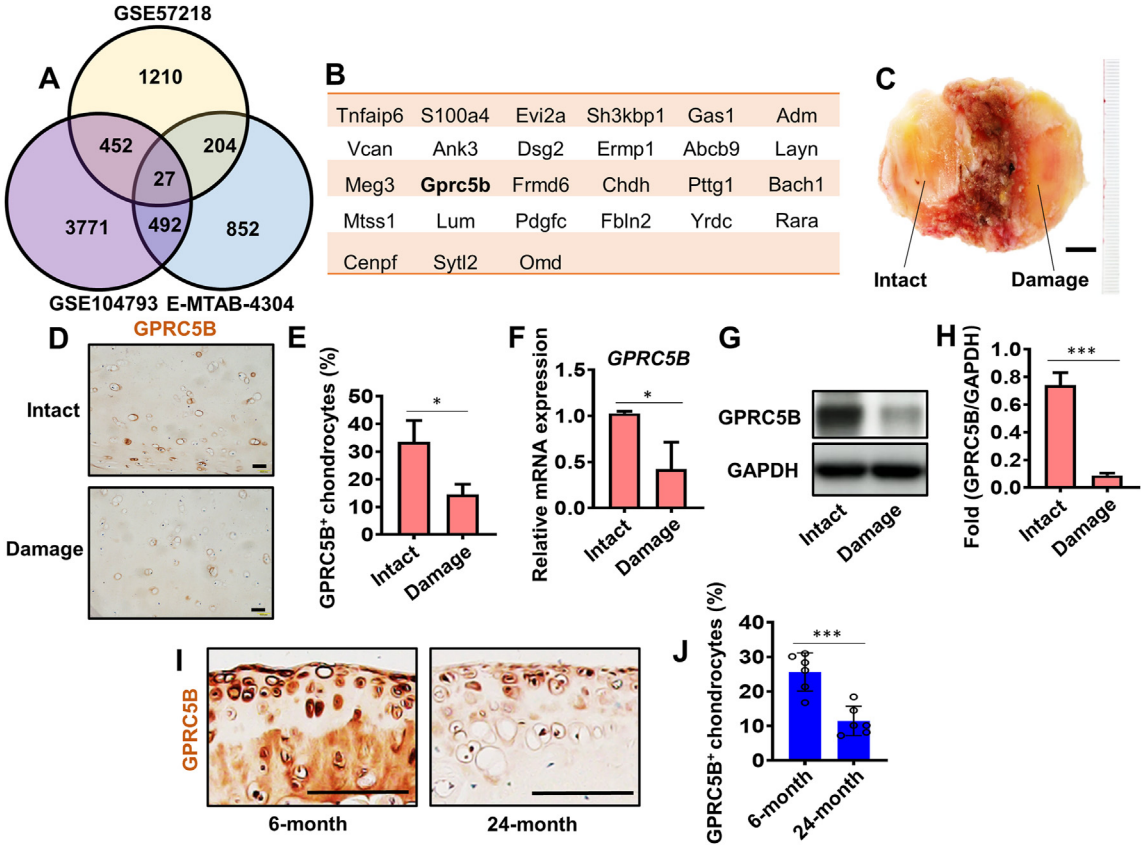

Figure 1 The expression of GPRC5B is associated with osteoarthritis. (A) Venn diagram of the different-expressing genes in GSE57218, GSE104793, E-MTAB-4304 datasets. (B) The names of overlapped 27 genes according to (A). (C) A representative image of the area of intact and damaged articular cartilage collected from the patients. Scale bar, 1 cm. (D) Representative IHC images for GPRC5B expression in damaged and intact articular from a clinical sample. Scale bar, 100 μm. (E) Percentage of GPRC5B^{+} chondrocytes in articular of samples shown in D. All data are presented as mean ± SD; $n = 3$; $^{*}P < 0.05$. Two-tailed Student's *t*-test was performed. (F) *GPRC5B* mRNA levels as determined by RT-qPCR in damaged and intact articular cartilage of patients. All data are presented as mean ± SD; $^{*}P < 0.05$. Two-tailed Student's *t*-test was performed with experiments repeated three times independently. (G) Representative images of Western blots for GPRC5B in damaged and intact articular cartilage from patient samples. (H) The quantified results of blots are shown in (G). Two-tailed Student's *t*-test was performed with experiments repeated three times independently. All data are presented as mean ± SD; $^{***}P < 0.001$. (I) Representative IHC images for GPRC5B expression articular cartilage of 6-month and 24-month-old mice. Scale bar, 50 μm. (J) Percentage of GPRC5B + chondrocytes in articular of samples shown in (I). All data are presented as mean ± SD; $n = 6$; $^{***}P < 0.001$. Two-tailed Student's *t*-test was performed.

there were no significant differences in synovitis between *Gprc5b*$^{-/-}$ and wild-type controls (Fig. 2F and G).

3.3. Gprc5b-deficiency enhances cartilage degradation and inhibits extracellular matrix (ECM) generation

We next investigated the effects of *Gprc5b*-deficiency on cartilage homeostasis by measuring expression of catabolic and anabolic genes in our DMM induced OA models. Our results indicate that chondrocyte hypertrophy marker COL10A1 and cartilage degradation marker MMP13 expression were robustly increased in articular cartilage of *Gprc5b*$^{-/-}$ mice compared to wild-type littermate controls (Fig. 3A–C). On the contrary, ACAN and COL2A1, the cartilage anabolic marker, was significantly decreased in articular cartilage of *Gprc5b*$^{-/-}$ mice (Fig. 3A, D and E). We next assessed expression of catabolic and anabolic proteins in different regions of the cartilage regions, include MTP and MFC. We found that chondrocyte hypertrophy markers COL10A1 and Runt-related transcription factor 2 (RUNX2), cartilage degradation markers MMP13 and matrix metalloproteinase 3 (MMP3) were increased in MTP and MFC of *Gprc5b*$^{-/-}$ mice compared to wild-type littermate controls following DMM. In contrast, the cartilage anabolic markers (ACAN and COL2A1) were significantly lower in the MFC and MTP of *Gprc5b*$^{-/-}$ mice compared to wild-type littermate controls following DMM (Supporting Information Fig. S4A–S4G and S5A–S5G). There were no differences in the expression of these genes between the *Gprc5b*$^{-/-}$ and wild-type littermate controls in the sham operated group.

Furthermore, to estimate the effect of GPRC5B on cartilage homeostasis in an inflammatory environment, we isolated femoral heads from *Gprc5b*$^{-/-}$ and respective wild-type control mice and cultured them with TNF-α for three days. Histological analysis showed that the ECM loss was significantly increase in femoral heads of *Gprc5b*$^{-/-}$ mice compared to the wild-type controls (Supporting Information Fig. S6A and S6B). Expression of COL10A1 and MMP13 were also increased, whilst the expression of ACAN were significantly decreased in the femoral heads of *Gprc5b*$^{-/-}$ mice compared to wild-type controls (Fig. S6C–S6F).

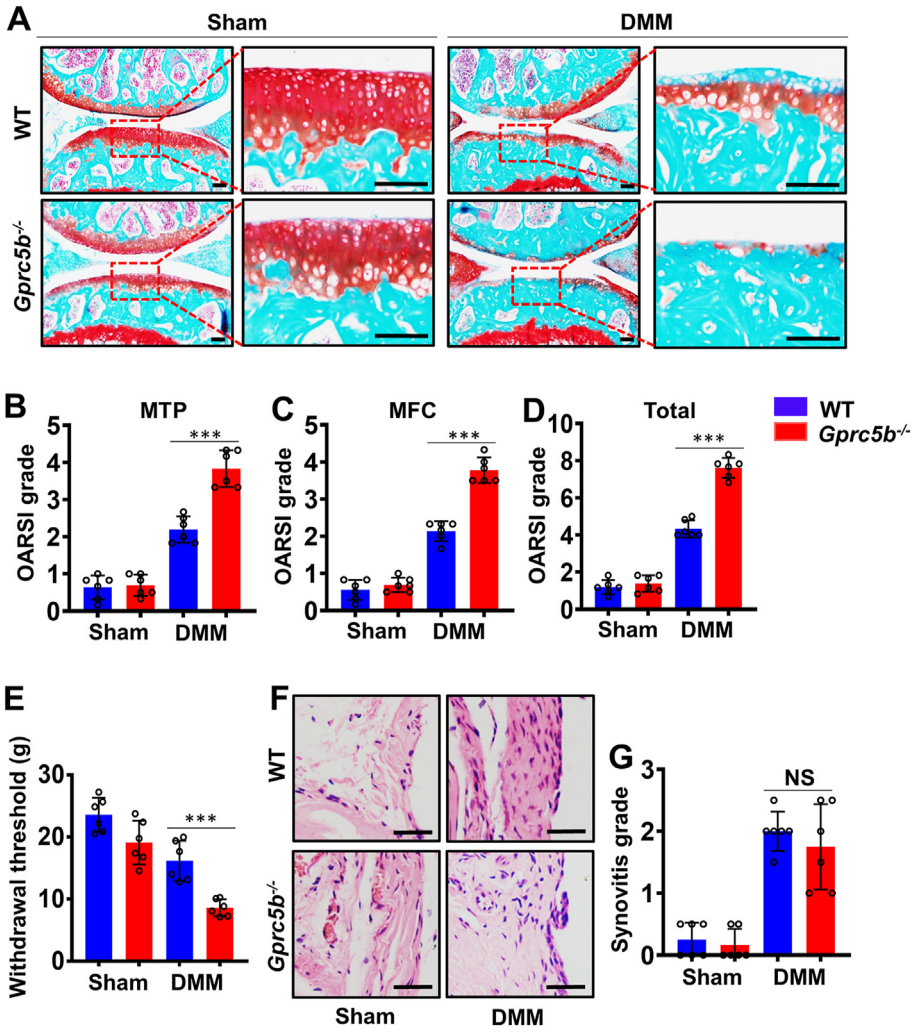

Figure 2 Ablation of *Gprc5b* aggravates OA pathogenesis in mice. (A) Representative images of safranin O/Fast green staining showing cartilage destruction after DMM surgery or control (sham) operation for 8 weeks. Scale bar, 100 μm. (B−D) The OARSI scoring of the medial tibia plateau (MTP) (B), medial femoral condyle (MFC) (C), Total scoring (MTP + MFC) (D). All data are presented as mean ± SD; $n = 6$; ***$P < 0.001$. Two-way ANOVA followed by Dunnett's test was performed for multiple comparisons test. (E) OA-associated pain was measured by the hot-plate assay. All data are presented as mean ± SD; $n = 6$; ***$P < 0.001$. Two-way ANOVA followed by Dunnett's test was performed for multiple comparisons test. (F) Representative H&E staining images of synovial inflammation. Scale bar, 100 μm. (G) The synovial inflammation scoring of DMM surgery or control (sham) operation. All data are presented as mean ± SD; $n = 6$; NS, not significant. Two-way ANOVA followed by Dunnett's test was performed for multiple comparisons test.

These results suggest a role of GPRC5B in cartilage homeostasis, especially in the setting of OA.

3.4. Overexpression of Gprc5b ameliorates OA pathogenesis in mice

To further validate the role of GPRC5B in OA, we overexpressed *Gprc5b* in mice by intra-articular injection of pLVX-IRES-*Gprc5b* lentivirus for 4 weeks after DMM operation, with intra-articular injection of the vector lentivirus (pLVX-IRES-Zsgreen lentivirus) serving as a control (Fig. 4A). Histological results suggest that the cartilage damage following DMM surgery was ameliorated in mice with *Gprc5b*-overexpressed compared to the vector controls (Fig. 4B). Indeed, this was reflected in the microscopic OARSI grading of MTP and MFC which showed that the articular cartilage damage was alleviated in mice that received the pLVX-IRES-*Gprc5b* lentivirus compared to those with the control vector lentivirus (Fig. 4C−E). The pain withdrawal threshold was also higher in mice that received the pLVX-IRES-*Gprc5b* lentivirus compared to the pLVX-IRES-Zsgreen lentivirus following DMM-induced OA (Fig. 4F).

Further immunohistochemistry analyses showed that COL10A1 and MMP13 expression was significantly decreased in articular cartilage of mice that received the *Gprc5b*-overexpression lentivirus compared to the control vector (Fig. 4G−I). In contrast, ACAN expression was elevated in articular cartilage of mice that received the *Gprc5b*-overexpression lentivirus compared to the control vector (Fig. 4G and J).

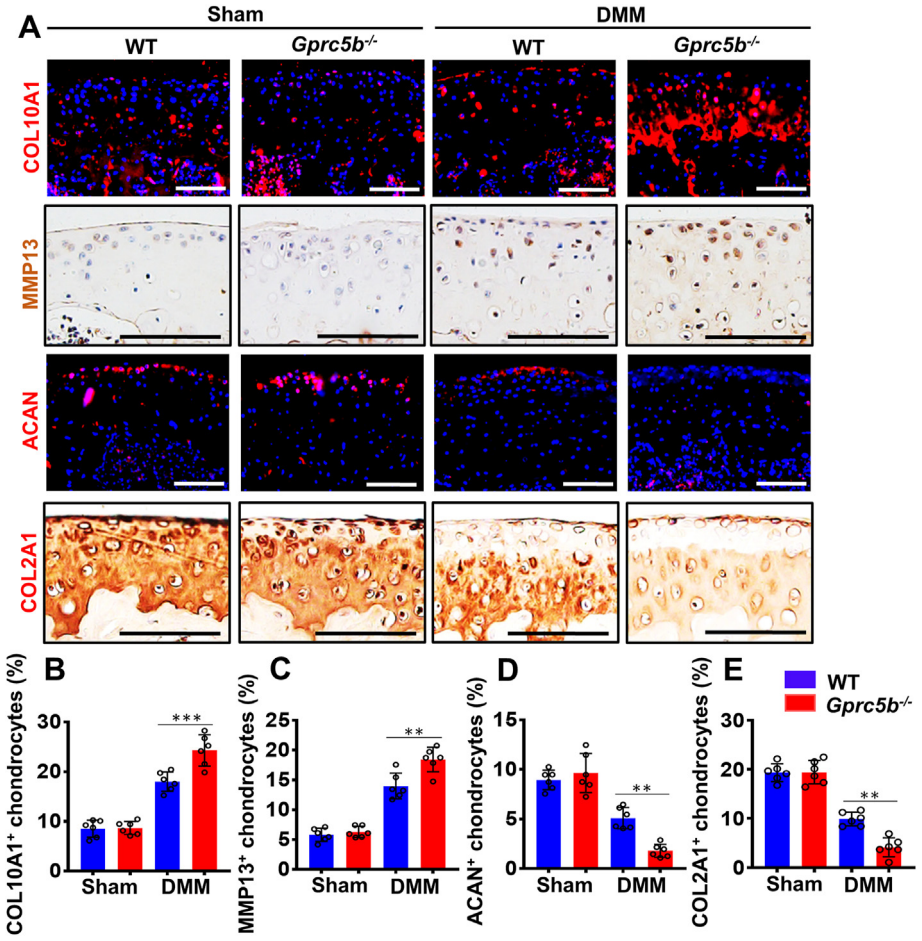

Figure 3 *Gprc5b*-deficiency enhances cartilage degradation and inhibits ECM generation. (A) Representative IF or IHC images for COL10A1, MMP13, ACAN and COL2A1 expression in articular cartilage of mice following DMM surgery or sham control operation after 8 weeks. Scale bar, 100 μm. (B−E) Percentage of COL10A1$^+$ (B), MMP13$^+$ (C), and ACAN$^+$ (D), COL2A1$^+$ (E) chondrocytes in articular of samples shown in (A). All data are presented as mean ± SD; $n = 6$; $^{**}P < 0.01$, $^{***}P < 0.001$. Two-way ANOVA followed by Dunnett's test was performed for multiple comparisons test.

3.5. Gprc5b ablation decreases cartilage anabolic genes expression and aggravates matrix metalloproteinase expression in vitro

We next investigated whether GPRC5B regulated TNF-α induced cartilage catabolic genes and anabolic genes expression *in vitro*. To do this, we isolated chondrocytes from the *Gprc5b*$^{-/-}$ and wild-type control mice and cultured them in presence of TNF-α for 24 h. Our results show that TNF-α-induced mRNA expression of *Mmp3*, *Mmp9*, and *Mmp13* were significantly upregulated in cells from *Gprc5b*$^{-/-}$ mice compared to those from wild-type control mice (Fig. 5A−C). This was accompanied by a decreased mRNA expression of *Acan*, *Col2α1* and *Sox9* (the cartilage anabolic genes) in the chondrocytes from *Gprc5b*$^{-/-}$ mice compared to wild-type controls (Fig. 5D−F). We also observed an increase in MMP13 and a decrease in ACAN protein expression, consistent with the above results (Fig. 5M−O).

We next overexpressed *Gprc5b* in ATDC5 cells and evaluated its effect on cartilage catabolic and anabolic gene expression. The overexpression of *Gprc5b* in ATDC5 cells was validated by RT-qPCR (Supporting Information Fig. S7A). In presence of TNF-α, we observed that the catabolic genes expression including *Mmp3*, *Mmp9*, and *Mmp13* were significantly downregulated in *Gprc5b* overexpressing cells compared to vector controls (Fig. 5G−I). This was accompanied with an increase in expression of *Acan*, *Col2α1* and *Sox9* (the cartilage anabolic genes) in *Gprc5b* overexpressing cells compared to the vector controls (Fig. 5J−L). Additionally, the expression of cartilage catabolic genes was inversely associated with the concentration of *Gprc5b* plasmid transfected (Fig. S7B−S7D), whilst the expression of anabolic genes had a positive association (Fig. S7E−S7G). This suggests that the regulation of cartilage homeostasis by *Gprc5b* is not *via* a dose-compensation effect.

Taken together, these data demonstrate that GPRC5B has an essential role in regulating both production and degradation of the extracellular matrix by chondrocytes in the inflammatory environment characteristic of OA.

3.6. GPRC5B mediated cartilage homeostasis occurs via AKT-mTOR-autophagy signaling

To investigate the downstream molecular mechanisms that mediate the effects of GPRC5B in OA, we performed RNA-sequencing analysis of chondrocytes from *Gprc5b*-deficiency and

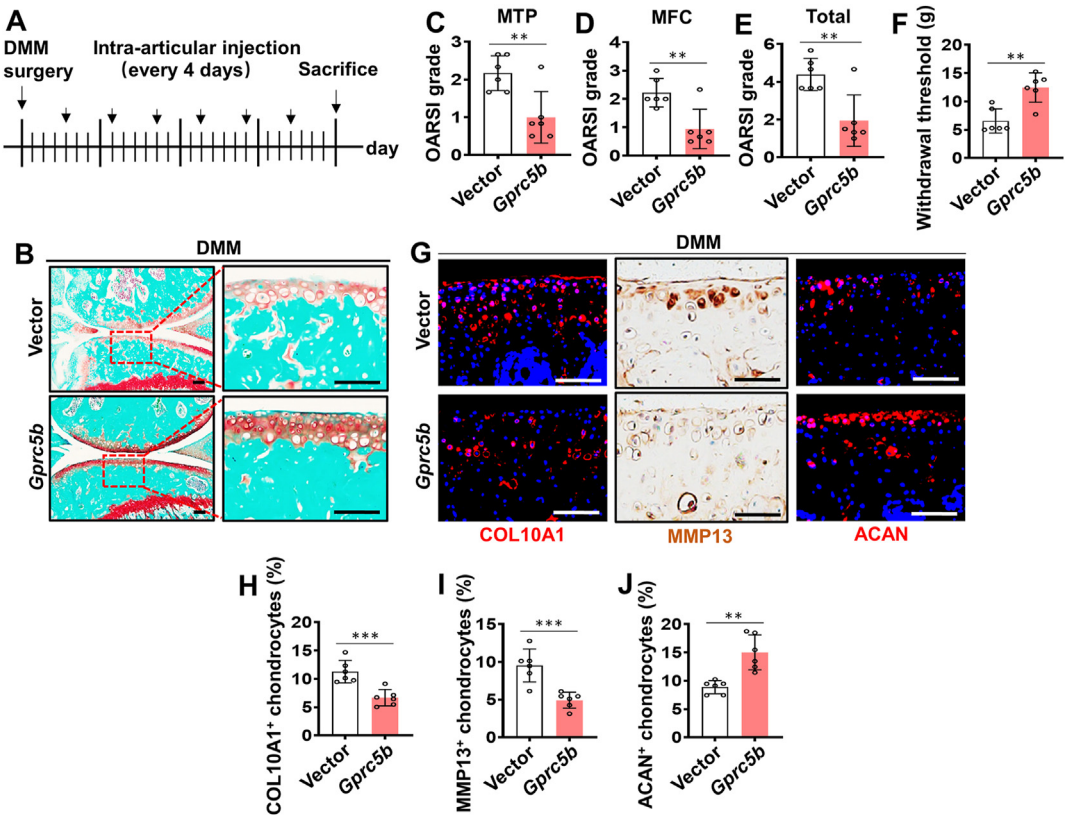

Figure 4 Overexpression of *Gprc5b* ameliorates OA pathogenesis in mice. (A) Experimental pattern for intra-articular injections of *Gprc5b* overexpression lentivirus vectors or vector controls. (B) Representative images of safranin O/Fast green staining showing cartilage destruction in *Gprc5b*-overexpression lentivirus injected mice and vector controls after DMM surgery. Scale bar, 100 μm. (C−E) The OARSI scoring of the medial tibia plateau (MTP) (C), medial femoral condyle (MFC) (D), total scoring (MTP + MFC) (E). All data are presented as mean ± SD; $n = 6$; $^{**}P < 0.01$. Two-tailed Student's *t*-test was performed. (F) OA-associated pain was measured by the hot-plate assay. All data are presented as mean ± SD; $n = 6$; $^{**}P < 0.01$. Two-tailed Student's *t*-test was performed. (G) Representative IF or IHC images for COL10A1, MMP13 and ACAN expression in articular cartilage of mice injected with *Gprc5b*-overexpression lentivirus vectors or vector controls after DMM surgery. Scale bar, 100 μm. (H−J) Percentage of COL10A1$^+$ (H), MMP13$^+$ (I), and ACAN$^+$ (J) chondrocytes in articular of samples shown in (G). All data are presented as mean ± SD; $n = 6$; $^{**}P < 0.01$, $^{***}P < 0.001$. Two-tailed Student's *t*-test was performed with experiments for two groups comparisons test.

wild-type littermate control mice. The results identified alteration in the phosphatidylinositol3-kinase (PI3K)−AKT signaling, with most up-regulated genes in the *Gprc5b*$^{-/-}$ cells being enriched in this pathway (Fig. 6A), besides, the heatmap displayed many PI3K pathway related genes have higher expression in *Gprc5b* knockout cells (Fig. 6B), which is consist with the gene set enrichment analysis (GSEA) of this pathway (Fig. 6C). Because mTOR signaling is the mainly downstream of PI3K−AKT pathway, we next analyzed the mTOR pathway and their protein−protein interaction (PPI) from our RNA-sequencing data, the results show that GPRC5B could regulate many different signaling pathway *via* interacting with mTOR pathway. Strikingly, those different signaling proteins are important for regulating cartilage homeostasis, suggesting that GPRC5B plays a key role in osteoarthritis regulation (Fig. 6D).

To confirm whether GPRC5B affected cartilage homeostasis by PI3K−AKT signaling, we overexpressed *Gprc5b* in ATDC5 cells and assessed the phosphorylation of AKT and mTOR after TNF-α stimulation. Consistently, phosphorylation of AKT and mTOR was significantly suppressed in *Gprc5b* overexpressing cells (Fig. 7A−C). This was accompanied by no effect on the phosphorylation of p65 in the *Gprc5b* overexpressing cells (Supporting Information Fig. S8A and S8B). Moreover, p-p65 levels were higher in the cartilage of DMM mice compared to sham operated, but no differences observed between WT and *Gprc5b*-deficient mice for both the sham and the DMM groups (Fig. S8C and S8D). This further suggests that GPRC5B may regulate cartilage function *via* the AKT−mTOR pathway, and not the NF-κB signaling axis as reported in other organs or systems.

AKT−mTOR signaling has been previously described to regulate OA pathogenesis, and involved in autophagy of articular chondrocytes[23−25], we also found that many interactions protein of the mTOR pathway can regulate autophagy from our PPI results (Fig. 6D), suggesting that GPRC5B regulate OA pathogenesis *via* AKT−mTOR−autophagy signaling. Indeed, we observed autophagy markers BECN1 and LC3 was also increased in *Gprc5b* overexpressing cells compared to the vector controls under bafilomycin A1 treated, whilst SQSTM1 expression was decreased (Fig. 7D−G). Moreover, this increase in LC3 expression also observed *in vivo*, with articular cartilage of mice following DMM induced OA having higher expression in the group injected with *Gprc5b*-overexpression lentivirus compared to the vector controls (Fig. 7H and I). Conversely, the expression of LC3 was

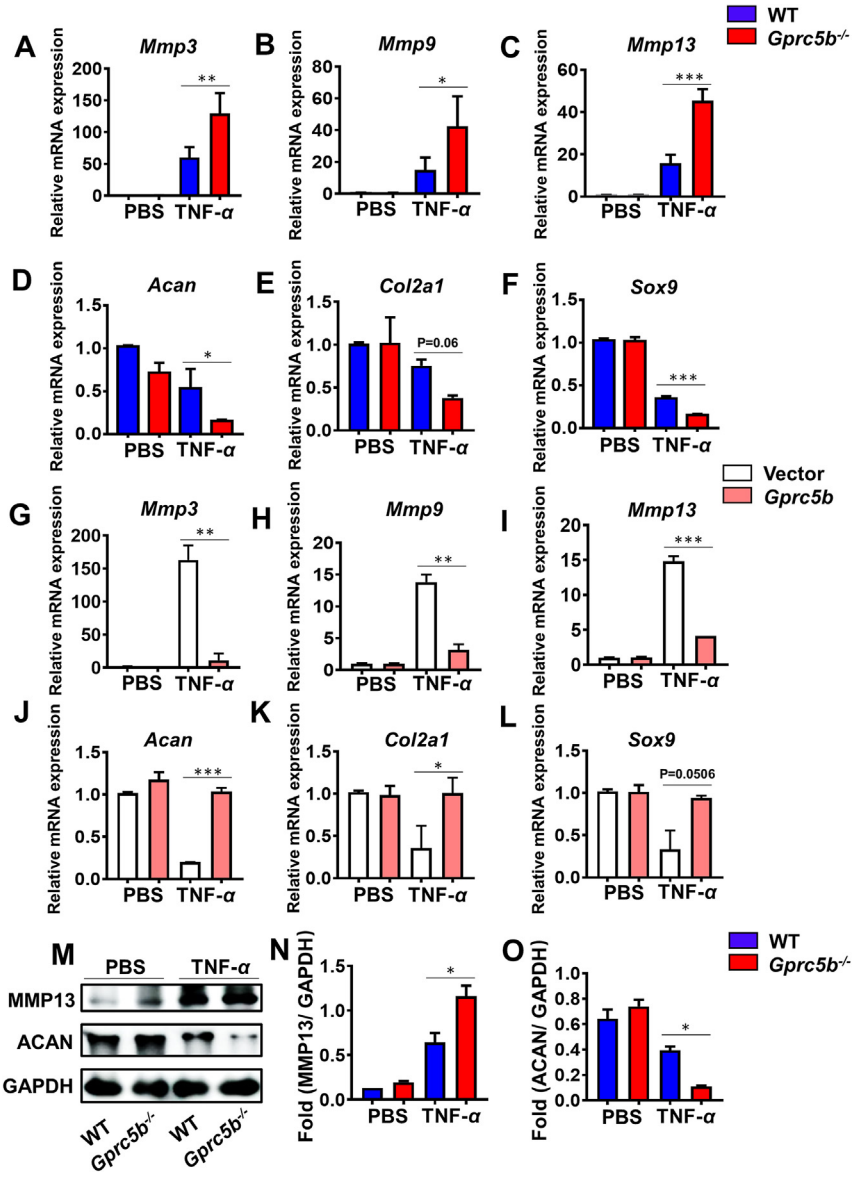

Figure 5 *Gprc5b* ablation decreases expression of cartilage anabolic genes and aggravates TNF-α-induced matrix metalloproteinase expression *in vitro*. (A−F) RT-qPCR analysis of *Mmp3*, *Mmp9*, *Mmp13*, *Acan*, *Col2α1* and *Sox9* mRNA levels in *Gprc5b*$^{-/-}$ and wild-type chondrocytes stimulated with TNF-α (10 ng/mL) for 24 h. All data are presented as mean ± SD; *$P < 0.05$, **$P < 0.01$, ***$P < 0.001$. Two-way ANOVA followed by Dunnett's test was performed for multiple comparisons test with experiments repeated three times independently. (G−L) RT-qPCR analysis of *Mmp3*, *Mmp9*, *Mmp13*, *Acan*, *Col2α1* and *Sox9* mRNA levels in vector control and *Gprc5b* overexpressing ATDC5 cells stimulated with TNF-α (10 ng/mL) for 24 h. All data are presented as mean ± SD; *$P < 0.05$, **$P < 0.01$, ***$P < 0.001$. Two-way ANOVA followed by Dunnett's test was performed for multiple comparisons test with experiments repeated two times independently. (M) Representative images of Western blots for MMP13 and ACAN in WT and *Gprc5b* deficient chondrocytes stimulated with TNF-α (10 ng/mL) for 24 h. (N, O) The quantified results of Western blots are shown in (M). All data are presented as mean ± SD; *$P < 0.05$. Two-way ANOVA followed by Dunnett's test was performed with experiments repeated two times independently.

significantly decreased in *Gprc5b*$^{-/-}$ mice in the DMM-induced OA mice model, compared to the littermate wild-type controls (Fig. 7J and K). We also observed that the expression of LC3 was significantly lower in damaged articular cartilage of patients compared to intact cartilage (Fig. 7L and M), and is consistent with our previous clinical observation for GPRC5B.

Finally, to investigate whether the regulation of cartilage homeostasis by GPRC5B occurred *via* autophagy signaling, we used chloroquine, an autophagy inhibitor widely utilized in cancer research[26]. We overexpressed *Gprc5b* in ATDC5 cells and stimulated them for 24 h with TNF-α, in presence or absence of chloroquine. We observed that under TNF-α stimulation for 24 h, the reduction of *Mmp3*, *Mmp9* and *Mmp13* mRNA levels mediated by *Gprc5b*-overexpression was blocked by chloroquine (Supporting Information Fig. S9A−S9C). Chloroquine also blocked *Gprc5b*-overexpression induced elevation in expression of *Acan*, *Col2α1* and *Sox9* (Fig. S9D−S9F). Furthermore, treatment with an mTOR antagonist rapamycin (RAPA), the increase in the expression of *Mmp3*, *Mmp9* and *Mmp13* and the reduction in expression of *Acan*, *Col2α1* and *Sox9* observed in *Gprc5b*-

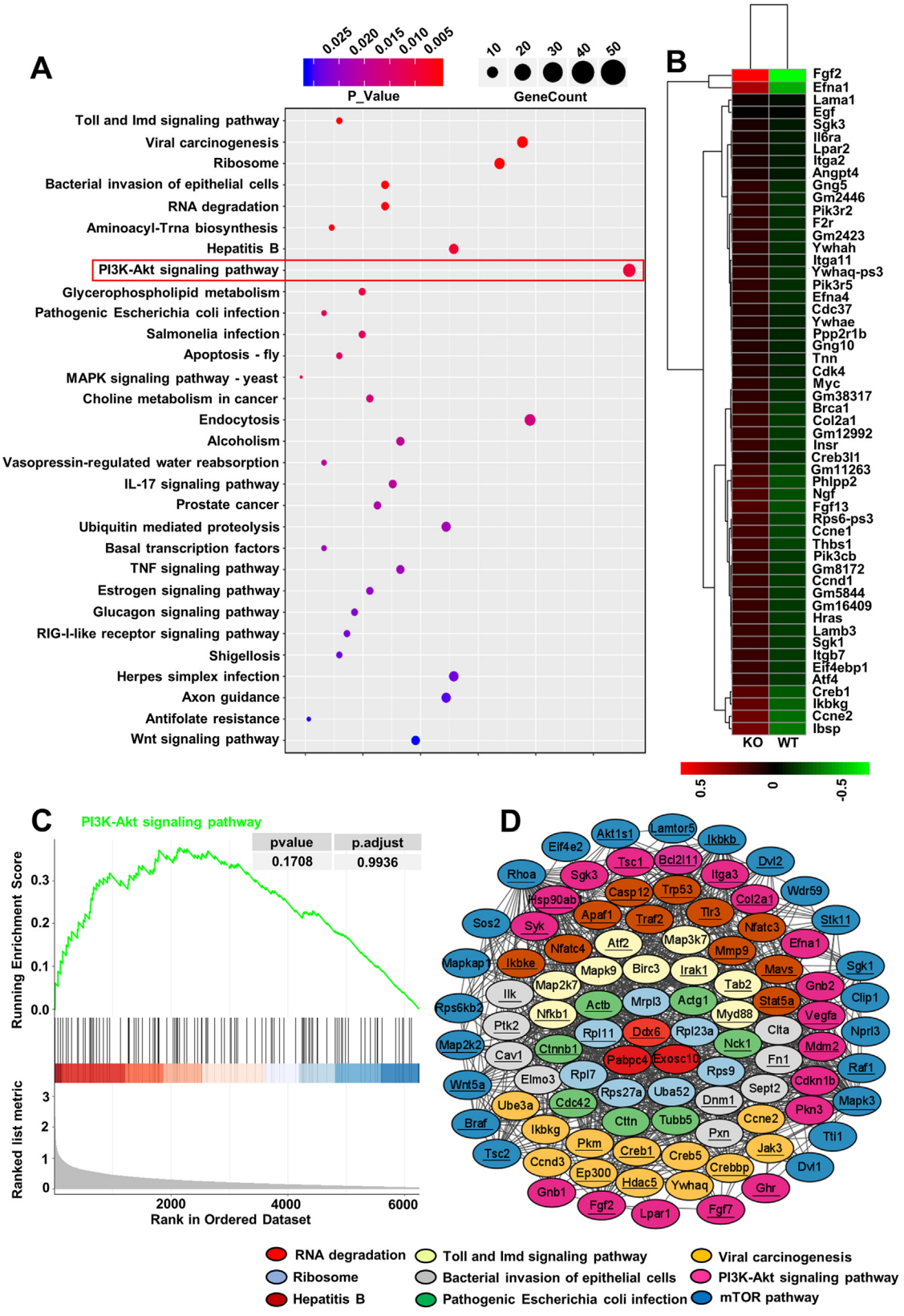

Figure 6 GPRC5B mediated cartilage homeostasis by PI3K−AKT signaling. (A) Kyoto Encyclopedia of Genes and Genomes (KEGG) pathway analysis of the wild-type and *Gprc5b*$^{-/-}$ chondrocytes stimulated with TNF-α (10 ng/mL) for 24 h in RNA-sequence analysis. (B) Heat map analysis related genes of PI3K−AKT pathway in wild-type and *Gprc5b*$^{-/-}$ chondrocytes stimulated with TNF-α (10 ng/mL) for 24 h. (C) The GSEA analysis showed that PI3k−Akt pathway is upregulation in *Gprc5b*$^{-/-}$ chondrocytes. (D) The PPI analysis of mTOR pathway from RNA-seq of wild-type and *Gprc5b*$^{-/-}$ chondrocytes. Blue is the mTOR pathway protein and their interaction protein has been summarized in the other eight pathways displayed by different colors. The underlined proteins are associated with autophagy signaling.

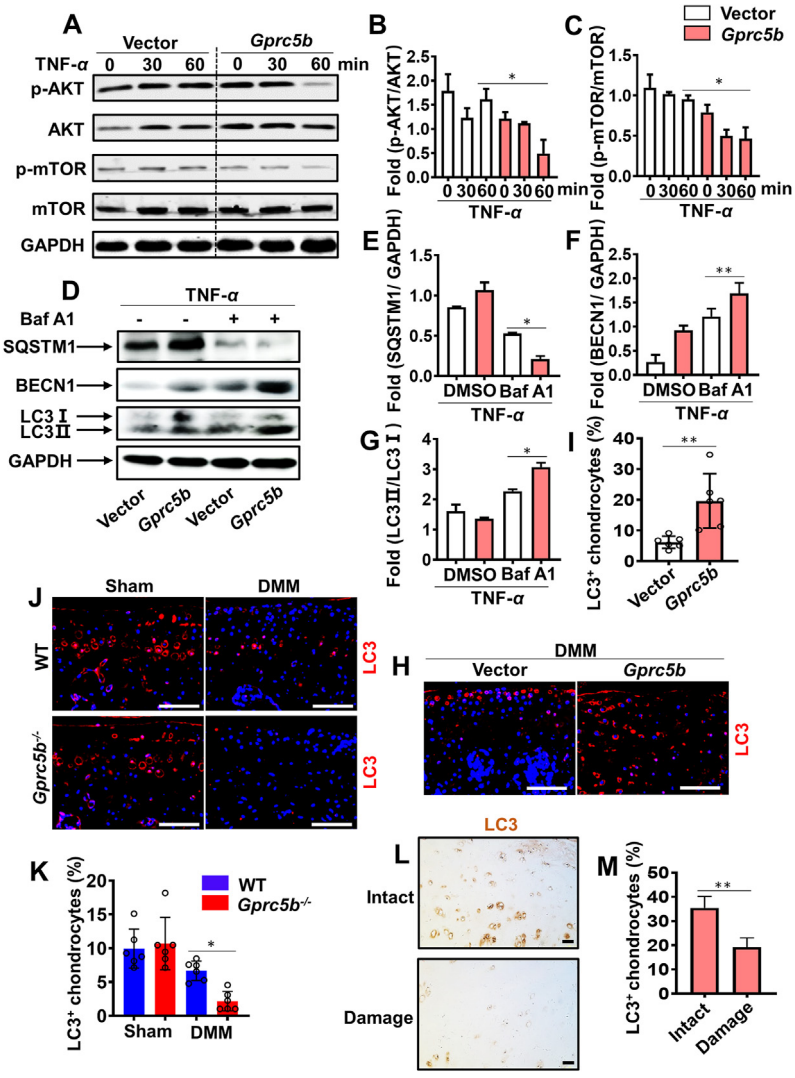

Figure 7 GPRC5B mediated cartilage homeostasis by AKT-mTOR-autophagy signaling. (A) Representative images of Western blots for p-AKT/AKT and p-mTOR/mTOR in *Gprc5b*-overexpressing and control vector ATDC5 cells, when treated with TNF-α (10 ng/mL) for the indicated time periods. (B, C) The quantified results of Western blots are shown in (A). All data are presented as mean ± SD; $^{*}P < 0.05$. Two-way ANOVA followed by Dunnett's test was performed with experiments repeated two times independently. (D) Representative images of Western blot of BECN1, SQSTM1 and LC3 in *Gprc5b* and control vector infected ATDC5 cells, when treated with TNF-α (10 ng/mL) and bafilomycin A1 (1 μmol/L) for 24 h. (E−G) The quantified results of Western blot blots are shown in (D). All data are presented as mean ± SD; $^{*}P < 0.05$, $^{**}P < 0.01$. Two-way ANOVA followed by Dunnett's test was performed with experiments repeated two times independently. (H) Representative IF images for LC3 expression in articular cartilage of mice injected with *Gprc5b*-overexpression lentivirus vectors or vector controls after DMM surgery. Scale bar, 100 μm. (I) Percentage of $LC3^{+}$ chondrocytes in articular of samples are shown in (H). All data are presented as mean ± SD, $n = 6$; $^{**}P < 0.01$. Two-tailed Student's *t*-test was performed. (J) Representative IF images for LC3 expression in articular cartilage of mice after DMM surgery or sham control operation after 8 weeks. Scale bar, 100 μm. (K) Percentage of $LC3^{+}$ chondrocytes in articular of samples are shown in (J). All data are presented as mean ± SD, $n = 6$; $^{*}P < 0.05$. Two-way ANOVA followed by Dunnett's test was performed for multiple comparisons test. (L) Representative IHC images for LC3 in damaged and intact articular cartilage from patient samples. Scale bar, 100 μm. (M) Percentage of $LC3^{+}$ chondrocytes in articular cartilage of samples are shown in (M). All data are presented as mean ± SD, $n = 3$; $^{**}P < 0.01$. Two-tailed Student's *t*-test was performed.

deficient chondrocytes under TNF-α stimulation, was blocked (Fig. S9G−S9L). Thus, these data indicate that GPRC5B may regulate cartilage homeostasis by the AKT−mTOR−autophagy signaling axis.

4. Discussion

Herein, we reported for the first time that GPRC5B may be a key regulator in OA progression. We demonstrated that the GPRC5B expression decreased during OA pathogenesis in human samples, and that *Gprc5b*-deficiency in mice aggravated the development of OA. Furthermore, ablation of *Gprc5b* was associated with enhanced expression of OA catabolic factors and decreased expression of the extracellular matrix molecules and cartilage anabolic genes. *Gprc5b* ablation also aggravated the TNF-α induced matrix metalloproteinase expression *in vitro*. Mechanistically, we found that in an inflammatory environment like OA, GPRC5B regulates chondrocyte function *via* the

AKT−mTOR−autophagy pathway. Lastly, we show that overexpressing *Gprc5b* ameliorates OA pathogenesis in mice by altering the cartilage homeostasis, and thus has a therapeutic potential to treat OA.

Osteoarthritis is a common disease that lacks an effective strategy to treat the underlying pathophysiology. Celecoxib, a current popular OA treatment, is used to relieve pain and inflammation but does not delay cartilage degeneration[27−29]. Other commonly used treatments such as glucosamine, chondroitin sulfate, and hyaluronic acid, are controversial in their ability to alleviate symptoms in OA patients[30,31]. Therefore, a drug target that can alleviate or even reverse the progression of OA remains an urgent unmet clinical need.

In OA pathological progression, disruption of cartilage homeostasis leads to subsequent ECM degradation[32]. Cartilage does possess a capacity for self-repair and regeneration by synthesizing ECM. Indeed, ECM regeneration plays a critical role in articular cartilage defects caused by traumatic injury[33,34]. In this study, we demonstrate that *Gprc5b* knock-out not only upregulated the expression of matrix-degrading enzymes, but also inhibited matrix synthesis and decreased expression of ECM-related genes (COL2A1 and ACAN) in articular cartilage. Moreover, overexpression of *Gprc5b* in the articular tissue improved COL2A1 and ACAN expression, reduced the expression of matrix-degrading enzyme in OA model. Thus, activation of GPRC5B presents a novel therapeutic target capable of promoting cartilage regeneration and thereby delaying OA progression.

GPCRs already account for ∼30% of FDA approved medicines, highlighting their vital role in disease and drug discovery, and further understanding of GPCR biology is warranted[35]. GPRC5B, a retinoic acid-induced gene, has been previously reported to affect macrophage infiltration and inflammatory cell recruitment through the NF-κB signaling pathway[13,14]. Moreover, GPRC5B activates obesity-associated inflammatory signals in adipocytes[36], and many studies on this gene focus on its correlation with inflammation[37,38]. OA is characterized by an inflammatory microenvironment, and therefore the role of GPRC5B in its progression is not wholly unexpected. However, we found that GPRC5B mediated cartilage homeostasis by the AKT−mTOR−autophagy pathway, and not the NF-κB signal pathway as previously reported (Fig. 5A−E).

Whilst our study highlights the potential of targeting GPRC5B for the treatment of OA, there are currently no known small-molecule agonists for the receptor. Here, we also show that increasing the expression of GPRC5B inhibits cartilage degradation, and increases cartilage regeneration *in vivo* and *in vitro*. With GPRC5B being a retinoic acid-induced gene, and in the absence of an available pharmacological intervention, increasing GPRC5B by retinoic-acid supplementation could be a possible therapeutic strategy. However, vitamin A and its metabolites appear to drive OA development[39], and therefore a small-molecule screen to identify a selective agonist for GPRC5B is warranted. Further research is also required to elucidate the other targetable molecules downstream of GPRC5B, and to identify the regulators of GPRC5B expression in chondrocytes, especially in response to TNF-α.

The present study has a few limitations. Whilst we demonstrate that GPRC5B mediated signaling improves cartilage anabolism and is protective against TNF-α-induced inflammatory cartilage degradation *in vitro* and *in vivo*, the role of GPRC5B expression in other cells in mediating these effects remains unexplored. Indeed, GPRC5B expression has been seen in a variety of cells including podocytes[13], vascular smooth muscle cells[40], fibroblast[14], and cerebellar Purkinje cells[41]. A cartilage-specific knockout of *Gprc5b* is warranted to further validate its role in OA progression. The DMM model for OA used in this study is most representative of OA development following traumatic joint injury[42,43]. The use of alternate traumatic OA models such as anterior cruciate ligament (ACL) rupture by tibia compression overloading or intra-articular tibia plateau fracture could be used to validate the findings observed here[44]. Furthermore, the role of GPRC5B in non-traumatic OA also remains to be explored. Here, we also made use of an overexpression system to elucidate the role of GPRC5B in OA pathogenesis due to the lack of a suitable ligand. It would be useful to conduct similar studies using small molecule agonists, especially to validate its potential as a therapeutic target.

Additionally, we have not shown how GPRC5B regulates the PI3K−mTOR pathway. However, there are many reports that do show PI3Kγ activation downstream of other GPCRs *via* the interaction of the G$\beta\gamma$ subunits to its p110γ catalytic and p101 regulatory subunits[45]. Other studies have indicated that constitutively active Gα subunits of the Gαq/11 and Gα12/13 may inhibit AKT activation[46]. Furthermore, β-arrestin have been shown to inactivate AKT and directly complex with PI3K catalytic subunit to restricts its enzymatic activity[47]. Therefore, there are a myriad of ways *via* which GPCR5B could regulate the PI3k−AKT−mTOR pathway, and further research would be required to better understand the predominant mechanism.

5. Conclusions

Our findings demonstrate that knocking out *Gprc5b* in mice elicits a more severe OA phenotype by upregulating cartilage catabolic factors and downregulating anabolic factor expression in a DMM-induced OA mouse model. Furthermore, we show that GPRC5B mediates these effects on cartilage homeostasis by regulating the AKT−mTOR−autophagy signal axis, and thus activation of GPRC5B could be a potential therapeutic target for delaying OA progression.

Acknowledgments

We are grateful to all members of the Jian Luo's lab for their technical help and discussion. This work is supported by grants from the National Key Research and Development Program of China (2020YFC2002800 and 2018YFC1105102 to Jian Luo), the National Natural Science Foundation of China (82225030, 92168204 and 9194910271 to Jian Luo), Shanghai Municipal Health Commission Excellent Young Medical Talents Training Program (2022XD034 to Jian Luo, China), the Fundamental Research Funds for the Central Universities (22120210586 to Jian Luo, China), and the East China Normal University (ECNU) Multifunctional Platform for Innovation (011).

Author contributions

Jian Luo, Mingyao Liu, Jian Fan supervised the projects and designed experiments. Liang He, Ziwei Xu, Xin Niu, Rong Li, Fanhua Wang, Yu You, Jingduo Gao performed the experiments and analyzed the data. Liang He and Karan M Shah wrote the manuscript. All of the authors have read and approved the final manuscript.

Conflicts of interest

The authors declare no conflicts of interest.

Appendix A. Supporting information

Supporting data to this article can be found online at https://doi.org/10.1016/j.apsb.2023.05.014.

References

1. Steinberg J, Southam L, Roumeliotis TI, Clark MJ, Jayasuriya RL, Swift D, et al. A molecular quantitative trait locus map for osteoarthritis. *Nat Commun* 2021;**12**:1309.
2. Global burden of 369 diseases and injuries in 204 countries and territories, 1990−2019: a systematic analysis for the Global Burden of Disease Study 2019. *Lancet* 2020;**396**:1204−22.
3. Ito Y, Matsuzaki T, Ayabe F, Mokuda S, Kurimoto R, Matsushima T, et al. Both microRNA-455-5p and -3p repress hypoxia-inducible factor-2 alpha expression and coordinately regulate cartilage homeostasis. *Nat Commun* 2021;**12**:4148.
4. Nuesch E, Dieppe P, Reichenbach S, Williams S, Iff S, Juni P. All cause and disease specific mortality in patients with knee or hip osteoarthritis: population based cohort study. *BMJ* 2011;**342**:d1165.
5. Butterfield NC, Curry KF, Steinberg J, Dewhurst H, Komla-Ebri D, Mannan NS, et al. Accelerating functional gene discovery in osteoarthritis. *Nat Commun* 2021;**12**:467.
6. Sun P, He L, Jia K, Yue Z, Li S, Jin Y, et al. Regulation of body length and bone mass by Gpr126/Adgrg6. *Sci Adv* 2020;**6**:eaaz0368.
7. Bassilana F, Nash M, Ludwig MG. Adhesion G protein-coupled receptors: opportunities for drug discovery. *Nat Rev Drug Discov* 2019;**18**:869−84.
8. Langenhan T. Adhesion G protein-coupled receptors-candidate metabotropic mechanosensors and novel drug targets. *Basic Clin Pharmacol Toxicol* 2020;**126**:5−16.
9. Luo J, Sun P, Siwko S, Liu M, Xiao J. The role of GPCRs in bone diseases and dysfunctions. *Bone Res* 2019;**7**:19.
10. Tomita H, Ziegler ME, Kim HB, Evans SJ, Choudary PV, Li JZ, et al. G protein-linked signaling pathways in bipolar and major depressive disorders. *Front Genet* 2013;**4**:297.
11. Tekola-Ayele F, Lee A, Workalemahu T, Sanchez-Pozos K. Shared genetic underpinnings of childhood obesity and adult cardiometabolic diseases. *Hum Genom* 2019;**13**:17.
12. Soni A, Amisten S, Rorsman P, Salehi A. GPRC5B a putative glutamate-receptor candidate is negative modulator of insulin secretion. *Biochem Biophys Res Commun* 2013;**441**:643−8.
13. Zambrano S, Moller-Hackbarth K, Li X, Rodriguez PQ, Charrin E, Schwarz A, et al. GPRC5b modulates inflammatory response in glomerular diseases *via* NF-kappaB pathway. *J Am Soc Nephrol* 2019;**30**:1573−86.
14. von Samson-Himmelstjerna FA, Freundt G, Nitz JT, Stelter F, Luedde M, Wieland T, et al. The orphan receptor GPRC5B modulates inflammatory and fibrotic pathways in cardiac fibroblasts and mice hearts. *Biochem Biophys Res Commun* 2019;**514**:1198−203.
15. Chung HJ, Kim JD, Kim KH, Jeong NY. G protein-coupled receptor, family C, group 5 (GPRC5B) downregulation in spinal cord neurons is involved in neuropathic pain. *Korean J Anesthesiol* 2014;**66**:230−6.
16. Saito T, Tanaka S. Molecular mechanisms underlying osteoarthritis development: notch and NF-kappaB. *Arthritis Res Ther* 2017;**19**:94.
17. Rigoglou S, Papavassiliou AG. The NF-kappaB signalling pathway in osteoarthritis. *Int J Biochem Cell Biol* 2013;**45**:2580−4.
18. Zhou F, Mei J, Han X, Li H, Yang S, Wang M, et al. Kinsenoside attenuates osteoarthritis by repolarizing macrophages through inactivating NF-kappaB/MAPK signaling and protecting chondrocytes. *Acta Pharm Sin B* 2019;**9**:973−85.
19. Neogi T. The epidemiology and impact of pain in osteoarthritis. *Osteoarthritis Cartilage* 2013;**21**:1145−53.
20. Nakamoto K, Nishinaka T, Sato N, Mankura M, Koyama Y, Kasuya F, et al. Hypothalamic GPR40 signaling activated by free long chain fatty acids suppresses CFA-induced inflammatory chronic pain. *PLoS One* 2013;**8**:e81563.
21. Glasson SS, Chambers MG, Van Den Berg WB, Little CB. The OARSI histopathology initiative—recommendations for histological assessments of osteoarthritis in the mouse. *Osteoarthritis Cartilage* 2010;**18**:S17−23.
22. Krenn V, Morawietz L, Haupl T, Neidel J, Petersen I, Konig A. Grading of chronic synovitis—a histopathological grading system for molecular and diagnostic pathology. *Pathol Res Pract* 2002;**198**:317−25.
23. Cai C, Min S, Yan B, Liu W, Yang X, Li L, et al. MiR-27a promotes the autophagy and apoptosis of IL-1 beta treated-articular chondrocytes in osteoarthritis through PI3K/AKT/mTOR signaling. *Aging (Albany NY)* 2019;**11**:6371−84.
24. Sun K, Luo J, Guo J, Yao X, Jing X, Guo F. The PI3K/AKT/mTOR signaling pathway in osteoarthritis: a narrative review. *Osteoarthritis Cartilage* 2020;**28**:400−9.
25. Xue JF, Shi ZM, Zou J, Li XL. Inhibition of PI3K/AKT/mTOR signaling pathway promotes autophagy of articular chondrocytes and attenuates inflammatory response in rats with osteoarthritis. *Biomed Pharmacother* 2017;**89**:1252−61.
26. Kimura T, Takabatake Y, Takahashi A, Isaka Y. Chloroquine in cancer therapy: a double-edged sword of autophagy. *Cancer Res* 2013;**73**:3−7.
27. Hochberg MC, Martel-Pelletier J, Monfort J, Moller I, Castillo JR, Arden N, et al. Combined chondroitin sulfate and glucosamine for painful knee osteoarthritis: a multicentre, randomised, double-blind, non-inferiority trial *versus* celecoxib. *Ann Rheum Dis* 2016;**75**:37−44.
28. Puljak L, Marin A, Vrdoljak D, Markotic F, Utrobicic A, Tugwell P. Celecoxib for osteoarthritis. *Cochrane Database Syst Rev* 2017;**5**:CD009865.
29. Somakala K, Amir M. Synthesis, characterization and pharmacological evaluation of pyrazolyl urea derivatives as potential anti-inflammatory agents. *Acta Pharm Sin B* 2017;**7**:230−40.
30. Simental-Mendia M, Sanchez-Garcia A, Vilchez-Cavazos F, Acosta-Olivo CA, Pena-Martinez VM, Simental-Mendia LE. Effect of glucosamine and chondroitin sulfate in symptomatic knee osteoarthritis: a systematic review and meta-analysis of randomized placebo-controlled trials. *Rheumatol Int* 2018;**38**:1413−28.
31. Bowman S, Awad ME, Hamrick MW, Hunter M, Fulzele S. Recent advances in hyaluronic acid based therapy for osteoarthritis. *Clin Transl Med* 2018;**7**:6.
32. Krishnan Y, Grodzinsky AJ. Cartilage diseases. *Matrix Biol* 2018;**71−72**:51−69.
33. Marijnissen AC, Lafeber FP. Re: E. B. Hunziker. Articular cartilage repair: basic science and clinical progress. A review of the current status and prospects. Osteoarthritis and Cartilage 2002; 10: 432-463. *Osteoarthritis Cartilage* 2003;**11**:300−463. author reply 2-4.
34. Cucchiarini M, Madry H. Biomaterial-guided delivery of gene vectors for targeted articular cartilage repair. *Nat Rev Rheumatol* 2019;**15**:18−29.
35. Hauser AS, Attwood MM, Rask-Andersen M, Schioth HB, Gloriam DE. Trends in GPCR drug discovery: new agents, targets and indications. *Nat Rev Drug Discov* 2017;**16**:829−42.
36. Kim YJ, Sano T, Nabetani T, Asano Y, Hirabayashi Y. GPRC5B activates obesity-associated inflammatory signaling in adipocytes. *Sci Signal* 2012;**5**:ra85.
37. Kim YJ, Hirabayashi Y. Caveolin-1 prevents palmitate-induced NF-kappaB signaling by inhibiting GPRC5B-phosphorylation. *Biochem Biophys Res Commun* 2018;**503**:2673−7.
38. Bauer D, Mazzio E, Soliman KFA. Whole transcriptomic analysis of apigenin on TNFalpha immuno-activated MDA-MB-231 breast cancer cells. *Cancer Genomics Proteomics* 2019;**16**:421−31.
39. Zheng XY, Liang J, Li YS, Tu M. Role of fat-soluble vitamins in osteoarthritis management. *J Clin Rheumatol* 2018;**24**:132−7.
40. Carvalho J, Chennupati R, Li R, Gunther S, Kaur H, Zhao W, et al. Orphan G protein-coupled receptor GPRC5B controls smooth muscle contractility and differentiation by inhibiting prostacyclin receptor signaling. *Circulation* 2020;**141**:1168−83.

41. Sano T, Kohyama-Koganeya A, Kinoshita MO, Tatsukawa T, Shimizu C, Oshima E, et al. Loss of GPRC5B impairs synapse formation of Purkinje cells with cerebellar nuclear neurons and disrupts cerebellar synaptic plasticity and motor learning. *Neurosci Res* 2018; **136**:33−47.
42. Lorenz J, Grassel S. Experimental osteoarthritis models in mice. *Methods Mol Biol* 2014;**1194**:401−19.
43. Culley KL, Singh P, Lessard S, Wang M, Rourke B, Goldring MB, et al. Mouse models of osteoarthritis: surgical model of post-traumatic osteoarthritis induced by destabilization of the medial meniscus. *Methods Mol Biol* 2021;**2221**:223−60.
44. Bapat S, Hubbard D, Munjal A, Hunter M, Fulzele S. Pros and cons of mouse models for studying osteoarthritis. *Clin Transl Med* 2018;**7**:36.
45. Heldin CH, Lu B, Evans R, Gutkind JS. Signals and receptors. *Cold Spring Harbor Perspect Biol* 2016;**8**:a005900.
46. Wu EH, Tam BH, Wong YH. Constitutively active alpha subunits of G(q/11) and G(12/13) families inhibit activation of the pro-survival Akt signaling cascade. *FEBS J* 2006;**273**:2388−98.
47. Wang P, DeFea KA. Protease-activated receptor-2 simultaneously directs beta-arrestin-1-dependent inhibition and Galphaq-dependent activation of phosphatidylinositol 3-kinase. *Biochemistry* 2006;**45**: 9374−85.